Controlling defect and dopant concentrations in graphene by remote plasma treatments

John B. Mc Manus [1], Alison Hennessy[1], Toby Hallam[2], Niall McEvoy[1], Conor P.Cullen[1] and Georg S. Duesberg[*,3]

[1] School Chemistry, Centre for Research on Adaptive Nanostructures and Nanodevices (CRANN) and Advanced Materials and Bioengineering Research (AMBER), Trinity College Dublin, Dublin 2, Ireland
[2] School of Electrical and Electronic Engineering, Newcastle University, Newcastle upon Tyne, United Kingdom
[3] Institute of Physics, EIT 2, Faculty of Electrical Engineering and Information Technology, Universität der Bundeswehr, München, Germany

Received ZZZ, revised ZZZ, accepted ZZZ
Published online ZZZ (Dates will be provided by the publisher.)

Keywords graphene, plasma treatment, nitrogen doping, graphene transistor, CVD

This report details the controllable doping of graphene through post-growth plasma treatments. Defects are controllably introduced into the lattice using argon plasma, following this sample are exposed to ammonia/hydrogen plasma. During this nitrogen atoms get incorporated causing partial restoration of the graphene lattice. The damage levels are characterised by Raman and X-ray photoelectron spectroscopies. The incorporation of nitrogen into the graphene lattice provides significant n-doping. This is confirmed by the fabrication of graphene field-effect transistors which show clear n-type behaviour and mobilities not significantly less than those of pristine graphene. Thus this work demonstrates the viability of plasma treatments to reliably dope graphene.

1 Introduction Graphene has been extensively studied over the last 15 years and has paved the way for novel electronic devices based on 2D materials. Despite the growing realisation that graphene cannot live up to all of its heralded promise, it still has the ability to revolutionise numerous areas of research. Real strides have been made towards making graphene industrially relevant in areas such as electrocatalysis, biological sensors, fuel cells and field emission sources[1,2].

These applications require graphene to be modified and tailored to perform optimally. One of the fundamental ways to modify semiconductors is doping. While doping may be achieved in many ways, one large-scale, non-volatile approach is modification by exposure to plasma. Plasma treatments allow for controlled introduction of dopants or functionalities into the graphene without the need for wet chemical steps[2].

Most plasma treatments modify graphene by breaking sp^2 bonds, providing the opportunity for other atoms or functional groups to be incorporated into the lattice[3]. Mild plasma treatments have also been used to remove polymer residue and other contaminants from graphene's surface to improve its electrical properties, without causing large-scale damage[4].

A range of gases can be used to form the plasma depending on the desired outcome. Certain plasmas, such as argon, serve to simply introduce damage to the lattice, while others such as nitrogen or oxygen can substitute for a carbon atom, mimicking doping in 3D semiconductors.

Graphene treated with oxygen plasma becomes p-doped due the electron with-drawing nature of the bonded oxygen species, as outlined by Nourbaksh *et al.*[5]. At higher levels of oxygen functionalisation, the presence of a bandgap was also detected. The use of plasma to n-dope graphene with nitrogen atoms has previously been shown by a number of groups[6]. Kato *et al*. investigated the edge functionalisation and doping of graphene nanoribbons. They used room-temperature NH_3 plasma to controllably functionalise predominantly edge sites [7]. Zeng *et al.* used nitrogen plasma to

* Corresponding author: e-mail duesberg@unibw.de, Phone: +49 89 6004 4036, Fax: +49 89 6004 3877

change the work function of graphene through the introduction of increased concentrations of graphitic N, increasing the electron concentration[8]. Ammonia plasma has also been used to electron dope graphene. Lin *et al*. demonstrated doping of mechanically exfoliated graphene by post-growth exposure to ammonia plasma and characterised the C-N bond types present intensively[9].

In this report we follow the work of McEvoy *et al*. and focus on the plasma doping graphene with nitrogen in a controllable manner[10]. Our method involves a two-step process whereby we first introduce damage into the graphene lattice with argon plasma and then heal the defects and simultaneously dope the graphene with a combined NH_3/H_2 plasma. As the samples are situated downstream of the source, the plasma has lost much of its kinetic energy before interacting with the sample, ensuring limited damage. We systematically examine the defect creation and doping through Raman spectroscopy and X-ray photoelectron spectroscopy (XPS). Finally, the electrical properties of the argon damaged and doped samples are confirmed by graphene field effect transistor (GFET) device measurements.

2 Experimental

2.1 Graphene growth Graphene was grown using a method similar to that described previously [11];[12]. Briefly, graphene was grown by CVD on 25μm copper foil. The samples were placed in a tube furnace where the temperature is increased to 1035˚C under H_2 flow (50 sccm, 0.5 mbar). The samples were then annealed at this temperature for 60 minutes followed by a 30 minute growth phase with H_2 (5 sccm) and CH_4 (10 sccm) gas flow at ~0.25 mbar. The furnace was then cooled to room temperature under 3 sccm H_2 flow. The samples were transferred to Si/SiO_2 wafers by spinning on a PMMA layer and then etching the Cu foil in ammonium persulfate solution, the details of which can be found in [13].

2.2 Plasma treatment An R^3T TWR 2000T microwave radical generator was used to perform the plasma treatment of the graphene. During Argon plasma exposure the conditions were typically 200 sccm of Ar gas with a chamber pressure of ~2 Torr. While for the NH_3/H_2 plasma 50 sccm of each gas was used giving a pressure of ~1 Torr. Samples were positioned ~30 cm downstream of the plasma source meaning that no direct heating of the samples took place. Furthermore the generated ions are energetically relaxed by this point reducing surface damage.

2.3 Characterisation and analysis A Witec Alpha 300R with a 532 nm excitation laser, with a power of ~1 mW, was used to collect the Raman spectra shown herein. All Raman measurements were taken after samples were transferred to SiO_2 and using a spectral grating with 600 lines/mm and a 100x objective lens. Raman maps were generated by taking scans every 150 nm in the x and y directions, typically over an area of 20 x 20 μm. Spectra shown are averages over these maps, with ~10,000 spectra being used for each.

XPS spectra were taken using a VG Scientific ESCAlab Mk II system with an Al Kα x-ray source. An electron flood gun was used for charge compensation and the binding energy scale was referenced to the carbon 1s core-level at 284.5 eV. Core-level scans were recorded at an analyser pass energy of 15 eV. Analysis was performed using CasaXPS software. Spectral components were fitted using a Shirley background subtraction, appropriate line shapes. Relative atomic percentages were calculated using the relative sensitivity factors provided by the software CasaXPS.

All electrical measurements were carried out with a Janis probe station in vacuum (~10^{-5} mbar). GFET electrodes (Ti/Au 5/40 nm) were deposited after plasma treatment by electron beam evaporation and patterned using shadow masking.

3 Results and discussion The Raman spectrum of pristine, transferred graphene on SiO_2 is shown in **Error! Reference source not found.**(a). The primary features of the spectrum are sharp and well characterised 2D (~2680 cm^{-1}) and G (~1590 cm^{-1}) peaks. The 2D peak can be fitted with a single Lorentzian, FWHM 31cm^{-1}, in agreement with other reports of monolayer graphene with some defect-induced broadening [11,14]. The intensity ratio of the 2D to G peaks is ~1.2. This is less than the usually quoted value of above 2 for monolayer graphene, however this may be due to damage of the film during polymer transfer or doping from any remaining polymer residue[15]. These factors allow the conclusion that the graphene is predominantly monolayer in nature.

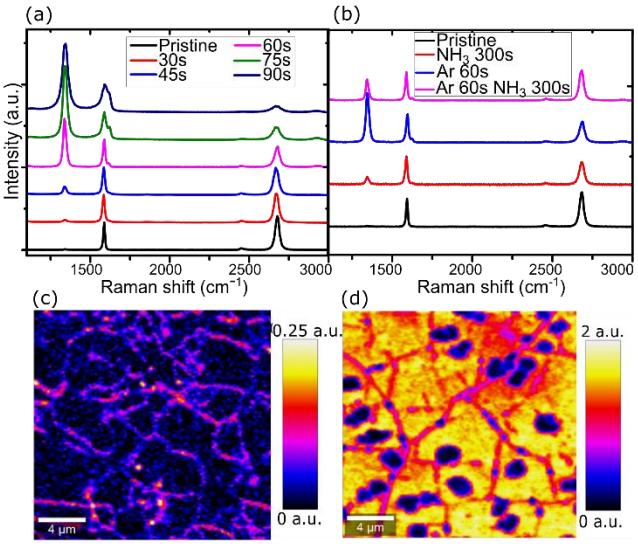

Figure 1 (a) Raman spectra of pristine graphene and after various exposure times of Ar plasma on SiO_2. All spectra are normalised to the G peak intensity. (b) Raman spectra of graphene treated by NH3/H2 and/or Ar plasma. All normalised to the G peak intensity. (c-d) Raman maps of pristine graphene and graphene after 60 seconds Ar exposure respectively.

In perfect sp^2 carbon systems, like graphene, the D peak is Raman forbidden. It becomes activated by a single-phonon intervalley scattering process, when momentum conservation is satisfied by the presence of defects[16]. The variation of D to G ratio with carbon crystalline size was first explored by Tuinstra and Koenig[17] and the ratio of the intensity of the D to G peak, $I_{D/G}$, is now often used as a measure of the defect density and quality of graphene. In this sample, the $I_{D/G}$ is less than 0.02 indicating the low defect level and high crystallinity of this monolayer sample[14].

The graphene samples were treated with downstream, argon plasma for different durations ranging from 30 to 90 seconds. The evolution of the Raman spectrum of graphene, scaled to the G peak intensity, is shown in **Error! Reference source not found.**(a). The most noticeable change is the dramatic increase in the intensity of the D peak with increasing plasma exposure. This indicates an increase in defect levels and is due to the plasma radicals damaging the graphene[16]. Examining the D to G ratio, $I_{D/G}$, it is found to increase gradually from below 0.2 to approximately 4 when the Ar exposure time is increased. This gradual increase is an attribute of the strong level of control possible in this system for introducing defects into monolayer graphene.

The 2D peak intensity is sensitive to electron scattering rates in the graphene. With increasing Ar exposure the 2D peak is observed to broaden and reduce in intensity, consistent with increasing defect concentration inducing higher scattering rates[18]. The D' peak (~1620 cm^{-1}) is also evident in the Raman spectra after more than 60 seconds of Ar plasma treatment. The D' peak is activated by a single-phonon intravalley scattering process, and, similar to the D peak, defects are required to satisfy momentum conservation. The ratio of the integrated areal intensity of the D to D', $A_{D/D'}$, can be related to the type of defects present in the sample[16]. When the D and D' peaks were fitted, $A_{D/D'}$ was found to be above 13, indicating the predominance of sp^3 type carbon defects in the sample.

Error! Reference source not found.(c-d) show Raman maps of the D to G peak intensity ratios of pristine graphene and graphene treated with 60 seconds of Ar plasma respectively. The pristine sample shows a very low $I_{D/G}$ intensity throughout, with the grain boundaries visible as the only areas showing any significant defect concentration. After 60 seconds in Ar plasma, the D peak intensity is greatly increased, the scale of this image is over an intensity range 8 times larger than that of the pristine sample. The areas of lowest intensity are bilayer islands which are much more resistant to plasma damage. Interestingly the grain boundaries are now also areas with lower $I_{D/G}$, in contrast to the image of the pristine graphene.

Plasmas have previously been used to successfully incorporate nitrogen atoms into the lattice of graphene[9,19]. However, the treatment of graphene by ammonia plasma alone forms very few substitutional N sites, and those which do form show a preference for edges and pre-existing defects, making it inappropriate as a general approach for doping[7]. NH_3/H_2 plasma, rather than NH_3 plasma alone was used as previous work had found that this plasma serves to heal defects in graphene while incorporating N atoms[10]. **Error! Reference source not found.**(b) shows the Raman spectra of samples treated with various combinations of Ar and NH_3/H_2 plasmas. In line with earlier reports, the spectra of the sample treated with 300 seconds NH_3/H_2 only has a small D peak component and marginally reduced 2D peak. For this reason pre-treating the graphene with Ar plasma, to introduce a controllable population of vacancy defects, was considered a suitable method to provide more available sites for incorporation of N atoms throughout the graphene, rather than predominantly at edge sites. As expected the sample becomes much more defective following Ar treatment, but notably, following the NH_3/H_2 plasma, the D peak intensity was reduced and the 2D peak was somewhat restored due to N atoms being incorporated into the lattice.

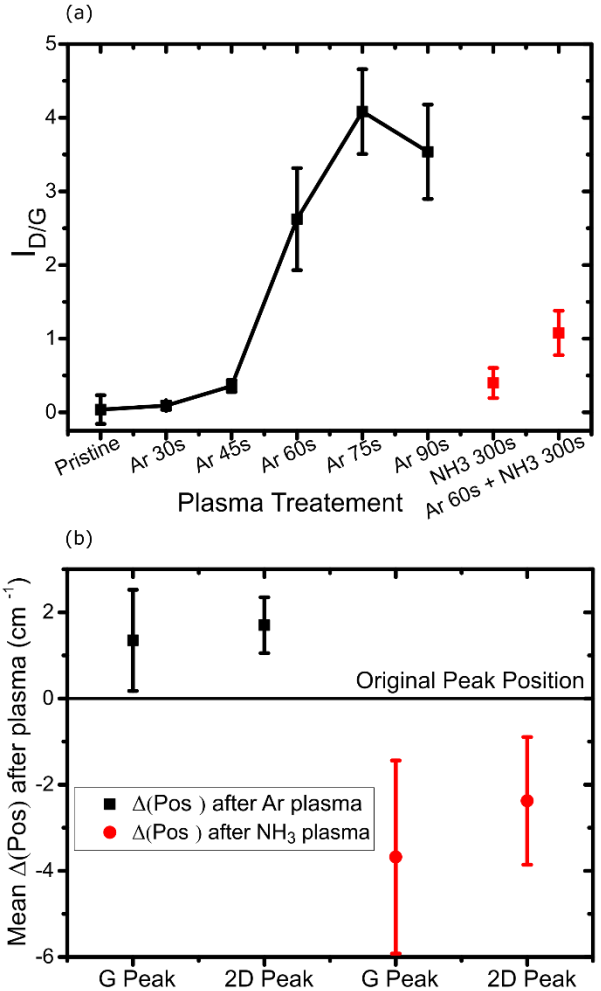

Figure 2 (a) Ratio of the Raman peak intensity of the D and G peaks, $I_{D/G}$, for different plasma exposures. (b) The average shift in peak position of the 2D and G Raman peaks after both Ar and NH_3/H_2 plasma treatments.

To allow further analysis of the Raman data after plasma exposure, certain peak behaviours were extracted and the trends plotted. Figure 2(a) shows the trend of Raman D to G peak intensity ratio for different plasma treatments. For the Ar plasma, the ratio increases gradually by over an order of magnitude, showing that the Ar plasma clearly causes controllable damage throughout the lattice, which can be tuned by modifying the plasma exposure time. The reduction in intensity for the 90s sample is consistent with the expected change in the relationship between the intensity of the D peak and the defect concentration at these defect levels.[20,21]. As previously discussed, the NH_3 causes comparably very little damage.

The shift in the Raman 2D and G peak positions are known to be an indicator of doping. Figure 2(b) shows the mean peak position shift of the G and 2D peaks after Ar plasma treatment, and subsequent NH_3/H_2 plasma. After Ar plasma the peaks reproducibly shift to higher wavenumbers. This is consistent with increased p-doping in the sample. When the samples are then exposed to the ammonia containing plasma, the peaks shift back to lower wavenumbers indicating a reduction of holes in the sample, or increased n-doping[22].

To gain a greater understanding of the influence of both plasma treatments on graphene, XPS was carried out on the above samples. Figure 3(a) shows the C 1s core level region for pristine graphene, graphene treated with 60s Ar plasma, and graphene treated with 60s Ar plasma followed by 300s NH_3/H_2 plasma. Analysis of the pristine, and Ar treated graphene shows a marked increase in non-sp^2 hybridised carbon species after plasma treatment, indicative of defect formation. It is clear that the Ar plasma treatment causes an increase in the contribution from sp^3 hybridised carbon atoms along with a large contribution from various carbon-oxygen species[23]. This could tentatively be attributed to the defective graphene sites oxidising when exposed to air between treatment and XPS analysis[24]. The third sample is exposed to argon and ammonia in succession with no exposure to air in between. While this sample also has an increase in sp^3 carbon, the contribution from carbon-oxygen species in this sample is significantly less than that for the Ar only treatment. The expected binding energy for C-N is also in this same region (within ~0.2eV), making deconvolution two difficult[25].

Due to the inability to reliable quantify any C 1s C-N component, the N 1s core-level region was also measured by XPS. The Ar and NH_3/H_2 treated sample contains an appreciable signal for of N at ~401 eV; which is consistent with quaternary N incorporated into the graphene lattice[26,27]. Neither the pristine nor Ar treated sample showed any significant signal in this region. Compositional analysis using the XPS data reveals a doping level of ~5at.% N. This is a strong indication of the incorporation of N atoms into the graphene lattice.

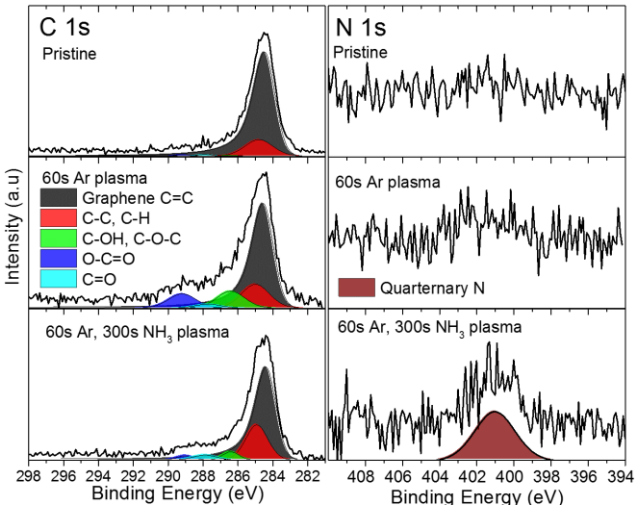

Figure 3 (a) C 1s XPS spectra of graphene samples exposed to no plasma, 60s Ar plasma, and 60s Ar and 300s NH_3/H_2 plasmas respectively. (b) XPS of the N 1s region of the same three samples

To analyse the effects of the plasma treatments on the electrical characteristics of the graphene, field effect transistors were fabricated, an image of one such device is shown in Figure 4(b). The two-terminal IV response of the pristine, Ar plasma treated and Ar and NH_3/H_2 plasma treated graphene are shown in Figure 4 (a) inset. Unsurprisingly, the pristine graphene has the lowest resistance as plasma treatments introduce defects and functional groups which would be expected to reduce conductivity[28]. We use the transfer characteristic of the devices, shown in **Error! Reference source not found.**Figure 4 (a), to extract the field-effect mobility. The pristine graphene shows an electron mobility of ~1200 $cm^2V^{-1}s^{-1}$ and a hole mobility of ~1500 $cm^2V^{-1}s^{-1}$. While these are lower than some reported previously for graphene [29,30], they are good values for back-gated CVD-grown graphene on SiO_2[31]. This sample is heavily p-doped with the Dirac point at ~48 V which we attribute to residual polymer and adsorbates[13].

The Ar plasma treated samples exhibit much reduced current levels and are strongly p-doped. For our devices the Dirac point is outside the measurement window of ±80V. This is in line with other studies which have found Ar plasma exposure serves to p-dope graphene[32]. In contrast the samples treated with Ar and NH_3/H_2 plasmas show a negative shift in the Dirac point. The Dirac point shifts by 45V to a value of 3V. Both of these are in line with the expected doping types indicated by position shift of the Raman peaks.

In addition to the doping, the gate response is restored after the ammonia treatment, indicating a partial healing of the lattice damage introduced by the argon. After this plasma treatment, the mobility is ~500 $cm^{-2}V^{-1}s^{-1}$ for both holes and electrons. This reduction, in comparison to the pristine values, is expected due to the damage caused by the

plasma treatments or by non-graphitic N atoms such as pyridinic and pyrrolic N.. However, it is a significant improvement from that seen after Argon damage alone which gave hole mobilites below 50 $cm^{-2}V^{-1}s^{-1}$. For samples less heavily p-doped before treatment, Figure 4(c), the Ar and NH_3/H_2 plasma treatments shift the Dirac point from ~20V to ~-25V, switching the graphene character from p-doped to an equivalent level of n-doping.

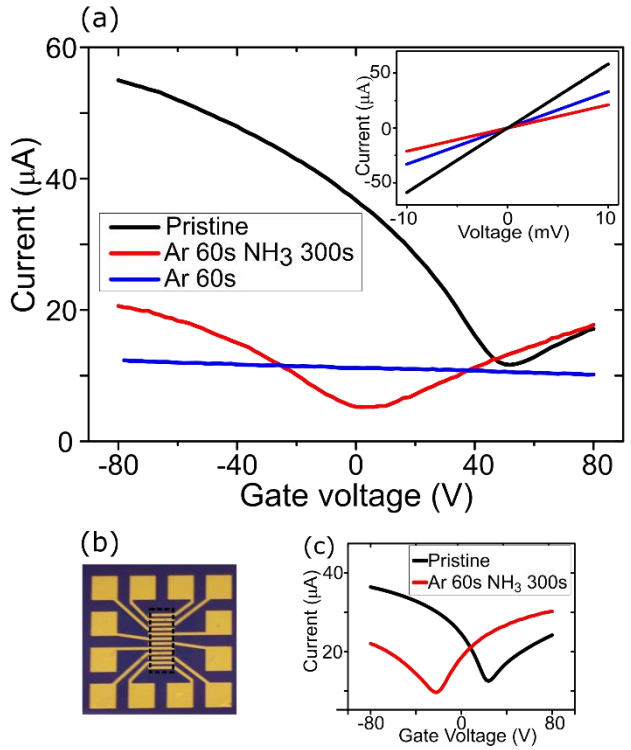

Figure 4 (a) Gate voltage sweeps of pristine, Ar treated and Ar NH_3/H_2 treated graphene samples, V_{DS} = 5mV. Inset: two-terminal IV measuremnts of the same samples. (b) Picture of the GFET device structure with graphene outlined. (c) Transfer curve of GFET device before and after plasma treatments indicating the switch from p- to n-type doping.

The electrical results demonstrate that the plasma treatments cause a shift of the Dirac point by 45 to 50V after treatment. This shift is consistent across multiple samples irrespective of the starting level of p-doping as was seen in Figure 4. All devices show a Dirac point shift of 45-50V which is equivalent to a doping level change of ~3.5 x 10^{12} cm^{-2}. This demonstrates the applicability of using plasma as a method to dope graphene. While there is some reduction in mobility values after plasma treatment, on the order of 50-60%, the mobility for both holes and electrons is still ~500 $cm^{-2}V^{-1}s^{-1}$. The ability to strongly and reproducibly modify the Dirac point position has the potential to outweigh the disadvantage of somewhat reduced mobility for many applications.

We have successfully used a remote Argon plasma to introduce a controllable concentrations of defects in monolayer graphene on SiO_2. This was confirmed through Raman and XPS analysis. The damaged graphene offered a platform for the subsequent use of NH_3/H_2 plasma to introduce nitrogen atoms to the graphene. The combined Ar and NH_3/H_2 plasma treatments provided reproducible electron doping of the graphene on the order of 10^{12} cm^{-2}. While further work is needed to understand the bonding configuration of the nitrogen atoms, this works provides clear evidence of the effectiveness of this two-step plasma doping to modulate the charge carriers in graphene.

Acknowledgements . J. B. Mc M. acknowledges an Irish Research Council scholarship, Project 204486, Award 13653. G. S. D. acknowledges the support of SFI under Contract No. 12/RC/2278 and PI_10/ IN.1/I3030. N. M. acknowledges support from SFI through 15/SIRG/3329.

References

[1] W. Choi, I. Lahiri, R. Seelaboyina, and Y. S. Kang, Critical Reviews in Solid State and Materials Sciences **35**, 52 (2010).
[2] A. Dey, A. Chroneos, N. S. J. Braithwaite, R. P. Gandhiraman, and S. Krishnamurthy, Applied Physics Reviews **3**, 021301 (2016).
[3] M. Meyyappan, Journal of Physics D: Applied Physics **44**, 174002 (2011).
[4] N. Peltekis, S. Kumar, N. McEvoy, K. Lee, A. Weidlich, and G. S. Duesberg, Carbon **50**, 395 (2012).
[5] N. Amirhasan *et al.*, Nanotechnology **21**, 435203 (2010).
[6] X. Wang, X. Li, L. Zhang, Y. Yoon, P. K. Weber, H. Wang, J. Guo, and H. Dai, Science **324**, 768 (2009).
[7] T. Kato, L. Jiao, X. Wang, H. Wang, X. Li, L. Zhang, R. Hatakeyama, and H. Dai, Small **7**, 574 (2011).
[8] Applied Physics Letters **104**, 233103 (2014).
[9] Y.-C. Lin, P.-Y. Teng, C.-H. Yeh, M. Koshino, P.-W. Chiu, and K. Suenaga, Nano Letters **15**, 7408 (2015).
[10] N. McEvoy, H. Nolan, N. Ashok Kumar, T. Hallam, and G. S. Duesberg, Carbon **54**, 283 (2013).
[11] X. Li *et al.*, Science **324**, 1312 (2009).
[12] S. Kumar *et al.*, physica status solidi (b) **248**, 2604 (2011).
[13] T. Hallam, N. C. Berner, C. Yim, and G. S. Duesberg, Advanced Materials Interfaces **1**, 1400115, 1400115 (2014).
[14] A. C. Ferrari *et al.*, Physical Review Letters **97**, 187401 (2006).
[15] DasA *et al.*, Nat Nano **3**, 210 (2008).
[16] A. Eckmann, A. Felten, A. Mishchenko, L. Britnell, R. Krupke, K. S. Novoselov, and C. Casiraghi, Nano Letters **12**, 3925 (2012).
[17] F. Tuinstra and J. L. Koenig, The Journal of Chemical Physics **53**, 1126 (1970).
[18] D. M. Basko, Physical Review B **78**, 125418 (2008).
[19] Applied Physics Letters **96**, 133110 (2010).
[20] M. M. Lucchese, F. Stavale, E. H. M. Ferreira, C. Vilani, M. V. O. Moutinho, R. B. Capaz, C. A. Achete, and A. Jorio, Carbon **48**, 1592 (2010).
[21] L. G. Cançado *et al.*, Nano Letters **11**, 3190 (2011).

[22] J. E. Lee, G. Ahn, J. Shim, Y. S. Lee, and S. Ryu, Nature Communications **3**, 1024 (2012).
[23] N. A. Kumar, H. Nolan, N. McEvoy, E. Rezvani, R. L. Doyle, M. E. G. Lyons, and G. S. Duesberg, Journal of Materials Chemistry A **1**, 4431 (2013).
[24] T. Larionova, T. Koltsova, E. Bobrynina, A. Smirnov, I. Eliseyev, V. Davydov, and O. Tolochko, Diamond and Related Materials **76**, 14 (2017).
[25] Y. Li, Z. Wang, and X.-J. Lv, Journal of Materials Chemistry A **2**, 15473 (2014).
[26] S. Hou, X. Cai, H. Wu, X. Yu, M. Peng, K. Yan, and D. Zou, Energy & Environmental Science **6**, 3356 (2013).
[27] Y. Zhang, Z. Sun, H. Wang, Y. Wang, M. Liang, and S. Xue, RSC Advances **5**, 10430 (2015).
[28] Y. V. Skrypnyk and V. M. Loktev, Physical Review B **82**, 085436 (2010).
[29] K. I. Bolotin, K. J. Sikes, Z. Jiang, M. Klima, G. Fudenberg, J. Hone, P. Kim, and H. L. Stormer, Solid State Communications **146**, 351 (2008).
[30] L. Banszerus *et al.*, Science Advances **1** (2015).
[31] O. M. Nayfeh, A. G. Birdwell, C. Tan, M. Dubey, H. Gullapalli, Z. Liu, A. L. M. Reddy, and P. M. Ajayan, Applied Physics Letters **102**, 103115 (2013).
[32] K. Thiyagarajan, B. Saravanakumar, and S.-J. Kim, ACS Applied Materials & Interfaces **7**, 2171 (2015).